Slow-Positron-Beam Techniques

The main advantage of the conventional sample–source sandwich arrangement is that the emitted positrons immediately penetrate the sample. A simple measurement arrangement in air is possible. The broad positron energy distribution up to 540 keV for ^{22}Na sources causes a relatively high maximum penetration depth. However, many problems in semiconductor physics are related to thin layers and to defects near the surface and at interfaces. The conventional techniques have only a limited applicability to such investigations. In order to obtain a defined small penetration depth, monoenergetic positrons (slow positrons) that can be set to defined energies by simple linear accelerators are necessary. Such setups are referred to as slow-positron-beam techniques throughout this book. They are elsewhere also called variable energy positron annihilation spectroscopy (VEPAS).

Monitoring of defects as a function of depth (defect depth profiling) is possible by adjusting the positron energy in a range of a few eV to several tens of keV. The monoenergetic positrons are obtained by moderation (Sect. 1). Only a small fraction of less than 1 % of incident positrons undergo this moderation process. The unmoderated positrons must be separated from the beam of monoenergetic positrons that is used for defect experiments after defined acceleration. The moderation requires the spatial separation of the source and the sample, and thus a beam guidance system must be used (Sect. 2). The measurement principles and the application for defect depth profiling of the different slow-positron-beam techniques are explained in Sects. 3 and 4.

1. Positron Source and Moderation

The energy emission spectrum of radioactive ^{22}Na sources is shown in Fig. 1. The moderation is based on the fact that a negative positron work function Φ_+ exists for many solids. In most cases, a transmission geometry with a thin moderator foil placed directly on top of the source capsule is used. The thickness of the foil is much smaller than the mean penetration depth and, therefore, only a small fraction of positrons thermalizes and starts to diffuse there. If the surface is reached during the diffusion, the positrons are spontaneously emitted from the moderator foil (Fig. 2) with a kinetic energy equal to the thermally broadened work function Φ_+. Materials with high atomic numbers are favorable for moderation, because the ratio of the mean diffusion length to the thermalization distance is larger. A suitable material is a single-crystal tungsten foil in a (100) orientation with a thickness of a few μm or a (110) tungsten single crystal for application in backscattering geometry. Since the positrons may be trapped in defects during their diffusion to the surface, a foil containing only a small number of positron traps must be prepared by annealing. The work function of a (110)-oriented tungsten single crystal was measured to be $\Phi_+ = -3.0$ eV and a moderation efficiency of 3×10^{-3} could be achieved (Vehanen et al. 1983). The moderation efficiency is given as the ratio of the number of moderated slow positrons to the total number of incident positrons. Routinely, efficiencies in the order of 10^{-4} can be obtained. Polycrystalline tungsten foils having an only slightly lower moderation efficiency have been also successfully tested (Brusa et al. 1992).

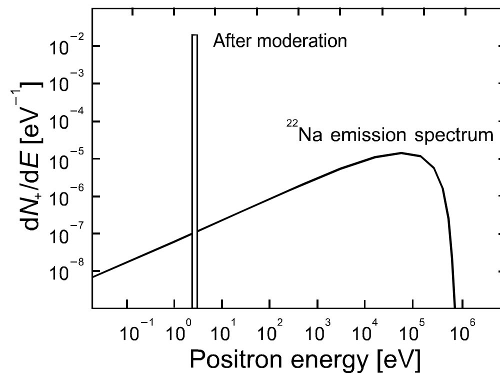

Fig. 1. Scheme of the positron emission spectrum of a ^{22}Na source. dN_+/dE is the number of positrons per energy channel E. The narrow curve centered at 3 eV illustrates the energy distribution after moderation in tungsten.

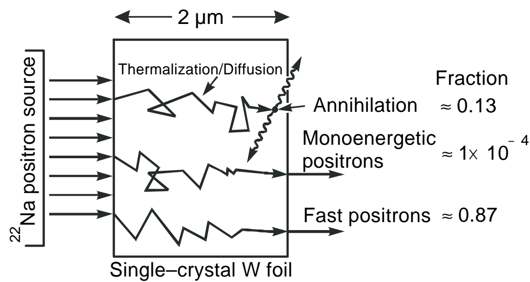

Fig. 2. Scheme of positron moderation in transmission geometry by a (100) tungsten foil. Most positrons leave the moderator foil with a high residual energy. A smaller fraction stops in the foil and annihilates there. When the surface is reached during diffusion, the positrons may be spontaneously emitted due to the negative work function of tungsten. The moderation efficiency amounts to about 10^{-4}.

Recently, solid-state rare-gas moderators, which are obtained by depositing a neon or krypton layer on a carrier foil at low temperatures, have been described (Khatri et al. 1990; Mills and Gullikson 1986). They have an extremely high efficiency, up to 10^{-2}, which cannot yet be conclusively explained. It is supposed that a drift due to an internal electric field superimposing the diffusive motion of the positrons plays an important role. Another future development may be the use of SiC as a field-assisted positron moderator (Bauer-Kugelmann et al. 1997; Beling et al. 1987; Brauer et al. 1997; Störmer et al. 1996a). This material is the only semiconductor known so far with a negative positron work function.

The low moderation efficiency requires much stronger positron sources for positron beam techniques than those used in conventional positron lifetime and Doppler-broadening spectroscopy. Intensive radiation protection is needed because the source activities are as high as 5×10^9 Bq (135 mCi).

2. Positron Beam Guidance Systems

The small fraction of monoenergetic positrons leaving the moderator must be separated from the unmoderated fraction before they can be utilized in experiments. This separation takes place in the beam guidance system by an energy filter, which may be realized in a magnetically guided system by internal electrodes in an **E**×**B** filter (Hutchings et al. 1986) or by applying external magnetic fields perpendicular to the beam direction (Liszkay et al. 1992). Another simple method is the use of bent solenoids. The unmoderated positrons are stopped in a shield. High vacuum conditions of 10^{-5} Pa are sufficient for the guidance system and positron studies near the sample surface. Ultra-high vacuum is only required in connection with surface studies. In this case, the specimen chamber should be separated by a differential pumping station. As an example, the

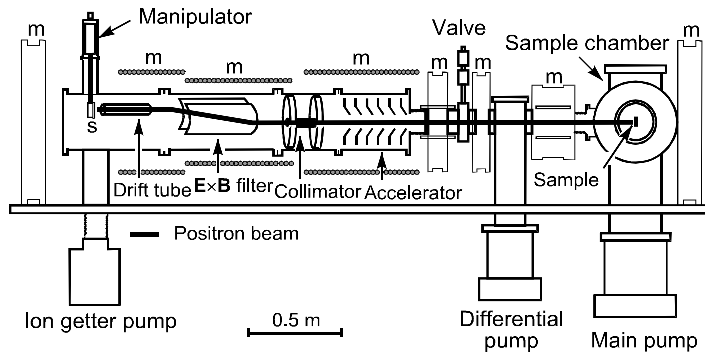

Fig. 3. Section view of the slow-positron-beam system POSSY at Martin Luther University Halle–Wittenberg. Positrons emitted from the source–moderator arrangement (s) are fed through the collimator by the **E**×**B** filter and are accelerated to the sample. The overall longitudinal magnetic field is generated by the guidance coils (m). The vacuum at the source side is kept in the 10^{-6} Pa range, while a pressure of 10^{-9} Pa may be achieved in the specimen chamber by means of the differential pumping stage.

magnetically guided positron beam system which is realized at Martin Luther University Halle–Wittenberg is shown in the section view of Fig. 3. The source–moderator arrangement is placed in front of a drift tube, at the end of which the positrons are entering the **E**×**B** filter. The monoenergetic positron beam is guided into the system axis and through a linear accelerator supplying a maximum energy of 50 keV. The fast positrons are stopped in the collimator.

The positron emission angle to the normal of the moderator foil amounts to a few degrees (Fischer et al. 1986). A longitudinal magnetic field, which is spread over the whole beam system, forces the positrons onto a helical trace. This ensures that all emitted slow positrons reach the target. A system of guidance coils (Fig. 3) generates this longitudinal field.

The beam guiding can also be done by a system of electrostatic lenses (Rosenberg et al. 1980). The main advantage is the possibility of focusing the beam. The design of such a lens system is, however, rather complicated due to the broad energy variation of the positron beam.

3. Measurement Principles

The Doppler-broadening technique can be applied for slow positrons similar to the conventional procedure with foil sources. The Ge detector is mounted close to the sample outside the specimen chamber. This is possible because the energy of the annihilation radiation is high enough to allow the transmission of the γ quanta through a thin stainless-steel wall. As explained earlier, the line shape parameters S and W can be used to identify defects and measure their concentration. In a

slow-positron system, these annihilation parameters are measured as a function of the positron beam energy, i.e. the implantation depth of the positrons. In addition to the depth sensitivity, another advantage of a slow-positron beam system is the quality of the Doppler spectra, as the birth γ-quanta in the source do not contribute to the background of the spectrum. Furthermore, there is no source contribution to the Doppler spectrum present in the conventional technique due to annihilations in the foil source.

The positron lifetime is much more powerful in the identification of the open volume of different defect types and the determination of concentrations compared with the Doppler-broadening technique. The conventional setup with start and stop detectors is not applicable in a slow-positron-beam system due to the strength of the source, since the start γ-quanta in the source cannot be correlated with annihilation events in the sample any more. Furthermore, the time of flight is much longer than the lifetime in the specimen. Thus, the measurement of the positron lifetime is only possible by pulsed beams supplying the start pulse by a specially designed bunching system. Such a technique is electronically expensive and has been realized up to now in only a few laboratories, e.g. in Munich (Kögel et al. 1988) and Tsukuba (Akahane et al. 1990). The performance limits of pulsed positron beams were discussed by Sperr and Kögel (1997).

In addition to lifetime and Doppler-broadening measurements, two-dimensional angular correlation of annihilation radiation can also be performed in a slow-positron-beam setup. The advantage is the analysis of the electronic structure at the surface, in thin epitaxial layers, or at interfaces (e.g. Howell et al. 1985; Peng et al. 1996).

The defect densities can be determined in a slow-positron system by a back-diffusion experiment in addition to the measuring principles of the momentum distribution and the positron lifetime. The fraction of positrons diffusing back to the surface, f_s, can be determined via the annihilation parameters at the surface or the fraction of positronium formed at the surface. This is possible because the surface annihilation parameters usually differ from the values in the interior of the sample, and positronium can usually only be formed at the semiconductor surface. The back-diffusing fraction of positrons is not only a function of the positron implantation depth and the diffusion constant, but also of the defect concentration. This is due to the fact that the trapped positrons cannot reach the surface. f_s is measured as a function of the incident positron energy. The corresponding fitting routines provide the trapping rate κ as a function of the depth. The main disadvantage of this procedure is that no information is available on the nature of the positron trap. Correlated positron lifetime measurements and Doppler-broadening measurements are recommended. On the other hand, total trapping rates for all positron traps are obtained by back-diffusion experiments. Hence, defect concentrations can also be determined in the case of saturated positron trapping, i.e. at very high concentrations, as was demonstrated for the case of ion-implanted silicon e.g. by Eichler et al. (1997a).

4. Defect depth profiling

In order to obtain the defect depth profile from the measured variation of annihilation parameters as a function of the incident positron energy, knowledge of the positron implantation profile is required. The profiles resulting from Monte-Carlo simulations and experimental results are presented in Sect. 4.1. The computation of the defect depth profiles is nowadays carried out with computer programs. These procedures are described in Sect. 4.2.

4.1 Positron Implantation Profile

In contrast to the conventional lifetime and momentum distribution techniques, the variation of the positron energy allows the detection of defects as a function of the penetration depth z, i.e. defect depth profiling. The implantation or penetration profile $P(z,E)$ of monoenergetic positrons having the energy E is given by

$$P(z,E) = \frac{mz^{m-1}}{z_0^m}\exp\left[-\left(\frac{z}{z_0}\right)^m\right] \quad \text{with} \quad z_0 = \frac{AE^r}{\rho\Gamma\left(1+\frac{1}{m}\right)}. \tag{1}$$

m, r, and A are empirical parameters. ρ is the mass density of the sample and Γ the gamma function. Widely used empirical values are: $A = 4.0\,\mu\mathrm{g\,cm^{-2}\,keV^{-r}}$, $m = 2$, and $r = 1.6$ (Vehanen et al. 1987).

$$\bar{z} = AE^r/\rho \tag{2}$$

represents the mean penetration depth. The positron implantation profile is called a Makhov profile, named after Makhov's original electron implantation experiments (Makhov 1961). The parameters of this profile can be obtained theoretically from Monte-Carlo simulations (Valkealahti and Nieminen 1983, 1984). Ghosh (1995) showed by several Monte-Carlo calculations that the parameters A and r are material dependent. The positrons after thermalization, i.e. at the beginning of diffusion, exhibit a depth distribution as given by (1). Examples of such Makhov profiles are shown in Fig. 4. The limitations of defect depth profiling for high positron energies become visible, as sharp defect structures lying relatively deep in the sample are smeared out when folded with the broad positron implantation profile. Ghosh (1995) obtained different A and r values depending on the Monte-Carlo schemes used. Although the main features of the positron implantation profile can be described by the analytical Makhov profile, small deviations are found. These deviations were the reason to approximate the profile obtained by Monte-Carlo simulations by a parameterized function (Ghosh and Aers 1995).

The empirical parameters of the Makhov profile (1) were also determined experimentally (Gebauer et al. 1997b; Leung et al. 1995). The results of the

former study are shown in Fig. 5. The parameters of the implantation profile could be determined from *S* versus *E* plots of amorphous silicon layers, since the thickness was determined independently by cross-section scanning electron microscopy (SEM). The a-Si layers of a thickness in the range 120 to 1000 nm were grown by molecular beam epitaxy on a SiO_2 buffer layer, which was obtained by thermal oxidation at 1000 °C. The *S* parameter curves were fitted using the VEPFIT program (see Sect. 4.2) using systematically varying *A* and *r* parameters of the Makhov profile. For every (*r*, *A*) pair, the mean quadratic deviation ξ was calculated from the deviation of the layer thickness obtained from the fit of the positron results, z_i^{fit}, and the layer thickness measured by SEM, z_i^{SEM},

$$\xi = \frac{1}{5}\sum_{i=1}^{5}\left(\frac{z_i^{\text{SEM}} - z_i^{\text{fit}}(A,r)}{z_i^{\text{SEM}}}\right)^2 . \tag{3}$$

The deviation ξ is averaged in (3) over all five measured *S*(*E*) profiles. Gebauer et al. (1997b) found a minimum deviation for the Makhov profile parameters of $A = (2.75 \pm 0.25)\ \mu\text{g cm}^{-2}\,\text{keV}^{-r}$ and $r = 1.7 \pm 0.05$, as can be seen in the contour plot of Fig. 5 b. These parameters are in a good agreement with the results of the Monte-Carlo simulation of Ghosh (1995).

4.2 Computation of Defect Depth Profiles

The positron trapping into defects can occur after thermalization during diffusion. The positron diffusion can be described as usual by the second Fick's law (compare Sect. 3.1.4). For the determination of depth profiles, only the one-dimensional diffusion equation has to be solved.

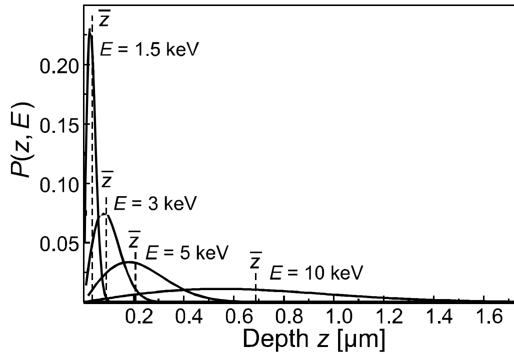

Fig. 4. Makhov profiles $P(z, E)$ in silicon calculated for four incident positron energies according to **Fehler! Verweisquelle konnte nicht gefunden werden.** with the parameters $A = 4.0\ \mu\text{g cm}^{-2}\,\text{keV}^{-r}$, $m = 2$, and $r = 1.6$. The dashed lines correspond to the mean penetration depth $\bar{z}$.

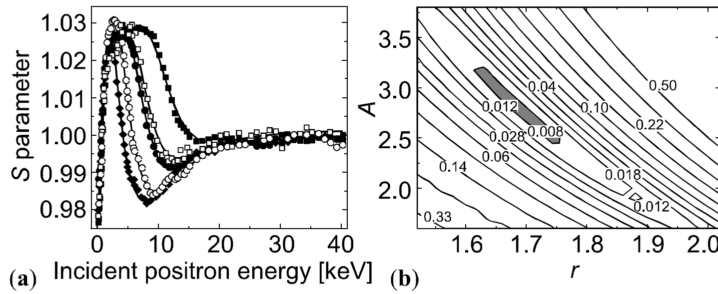

Fig. 5. Experimental determination of the parameters A and r of the Makhov profile (1). (**a**) S parameter as a function of the positron energy for amorphous silicon layers (■ 1000 nm, □ 485 nm, ● 350 nm, ○ 200 nm, ◆ 120 nm thickness) grown on 600 nm thick silicon dioxide. The oxide layer was obtained by 1000 °C annealing of a Czochralski-grown silicon wafer. The solid lines are numerical fits with the VEPFIT (variable energy positron fit) program. The A and r parameters were varied in order to reproduce the thickness of the Si layer determined independently by cross-section scanning electron microscopy (SEM). (**b**) Mean quadratic deviation ξ of the thickness determined from the positron experiment by VEPFIT and SEM shown as contour lines in an A versus r plot. The parameter A is given on the axis in units of $\mu g\, cm^{-2}\, keV^{-r}$. All five curves were taken into account for the calculation of ξ. The minimum deviation is indicated by the shaded area at $A = (2.75 \pm 0.25)\ \mu g\, cm^{-2}\, keV^{-r}$ and $r = 1.7 \pm 0.05$ (Gebauer et al. 1997b).

Possible quantities of the measurement are the line shape parameters (S or W parameter), the positron lifetime components τ_i and their intensities I_i, or the so-called positronium fraction F. The profile of these annihilation parameters in terms of the depth is the defect profile in the sample convolved by the penetration profile $P(z, E)$ and influenced by the positron diffusion. The diffusion equation must be solved numerically. However, the defect depth profile can hardly be identified directly. For the numerical procedure, the sample is usually divided into slices which are taken thin enough to assume a constant defect concentration and a constant positron density there. The annihilation parameters are fitted as a function of the energy in a non-linear procedure. In this way, the defect distribution perpendicular to the surface is obtained.

The VEPFIT[1] program is a package for the evaluation of slow-positron beam data (van Veen et al. 1990, 1995). A Gaussian curve as an analytical function of the defect profile or a simple slice structure with a constant defect concentration in the particular layer must be taken as a program input. Both a Gaussian and a step function of the defect concentration may reflect the experimental data appropriately. Often, it cannot be decided which function is the better choice to

[1] Variable energy positron fit.

mimic the real defect profile. This is due to the broad implantation profile of the positrons and the positron diffusion, which is itself a function of the defect concentration.

Another algorithm (POSTRAP program) for the evaluation of slow-positron depth profiles in order to carry out defect depth profiling was presented by Aers (1990). The program includes defects and the effect of electric field on positron diffusion. It allows arbitrary forms of the positron implantation profile.

An example of the determination of a defect profile is shown in Fig. 6. The *S* parameter was measured as a function of the positron implantation energy in arsenic-implanted silicon (Gebauer et al. 1995). The data were fitted using VEPFIT assuming a structure of four slices of different defect densities or a Gaussian-like defect distribution.

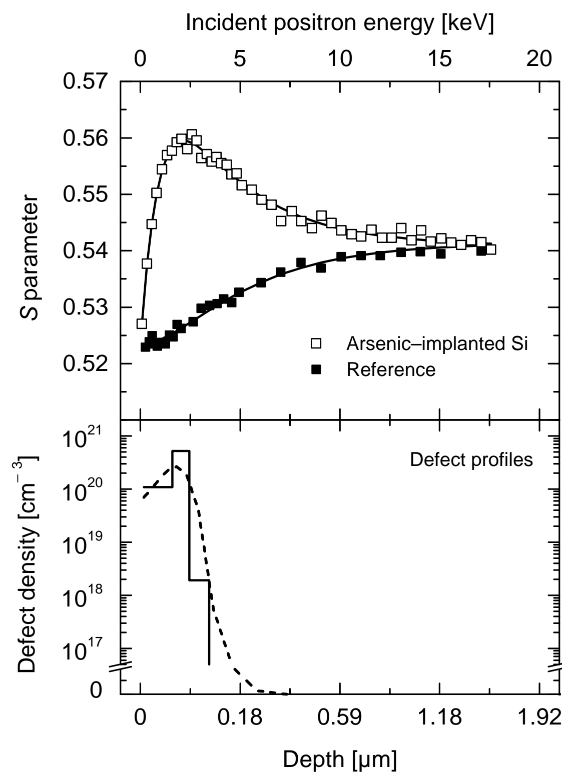

Fig. 6. *S* parameter as a function of the incident positron energy for a silicon sample implanted with 5×10^{13} cm^{-2} arsenic (60 keV). The curve through the data points was obtained by VEPFIT (variable energy positron fit). The data and the fit for as-grown Si free of positron traps are shown as reference. Four slices of different defect densities or a Gaussian-like defect distribution were assumed for the fit. The layer structure providing the best fit is shown in the lower panel (Gebauer et al. 1995).

The computer programs mentioned above also provide the fraction of positrons diffusing back to the surface, f_s. Such back-diffusion experiments have the advantage that the positron trapping rate can also be determined in the case of saturated positron trapping in defects, in contrast to the conventional techniques. This means that there is in principle no upper sensitivity limit. However, the lower sensitivity limit is comparable to the conventional techniques due to the requirement of a minimum fraction of positrons annihilating from defects. The annihilation fraction η can be calculated from f_s as a function of incident positron energy E, i.e. as a depth profile,

$$\eta(E) = 1 - \frac{f_s(E)}{f_s^{ref}(E)}, \quad (4)$$

where $f_s(E)$ are values in the sample under consideration and $f_s^{ref}(E)$ the corresponding back-diffusion fractions in a defect-free reference sample (Mäkinen et al. 1986).